

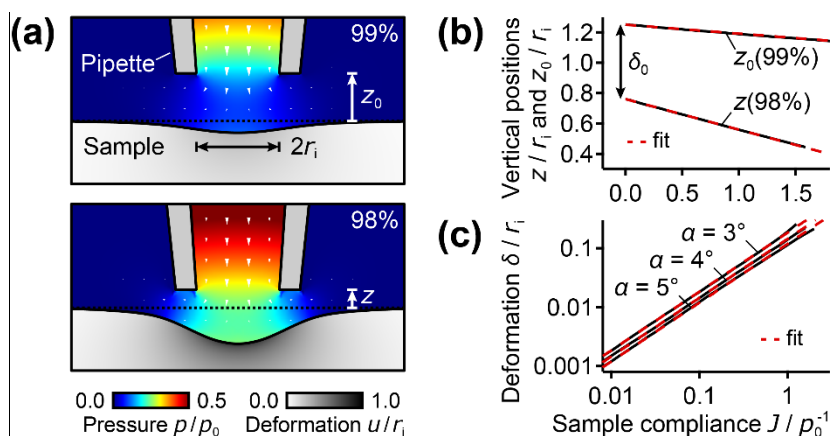
## Supplemental Material

### Mapping the creep compliance of living cells with scanning ion conductance microscopy reveals a subcellular correlation between stiffness and fluidity

J. Rheinlaender and T. E. Schäffer

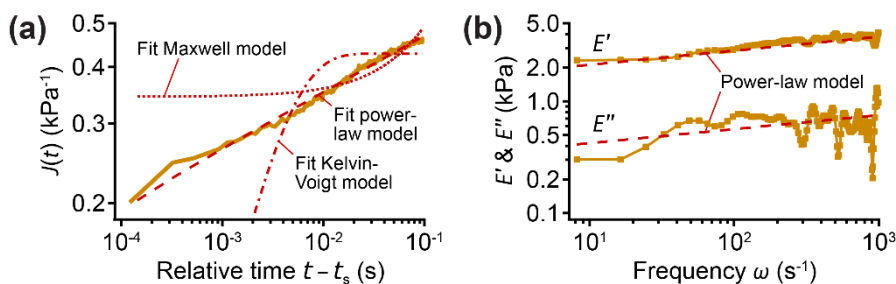
Institute of Applied Physics, University of Tübingen, Auf der Morgenstelle 10, 72076 Tübingen, Germany.  
E-mail: johannes.rheinlaender@uni-tuebingen.de & tilman.schaeffer@uni-tuebingen.de

#### Numerical Model



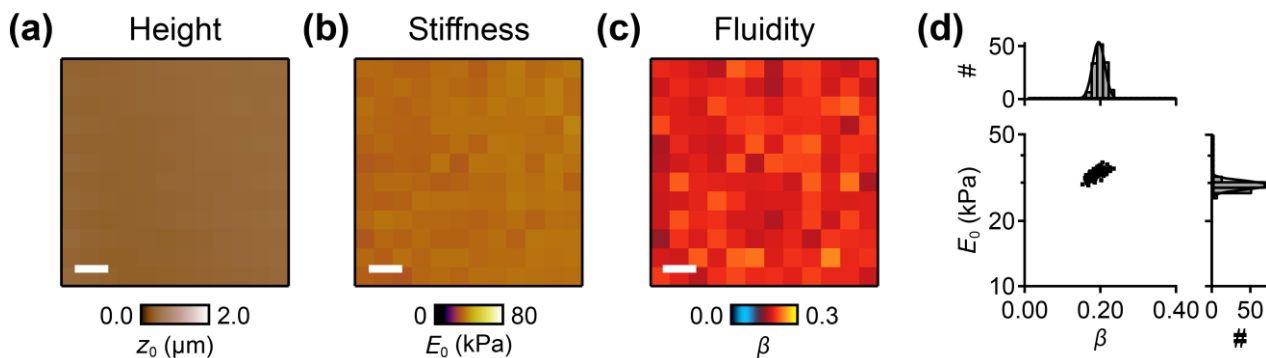
**Suppl. Fig. S-1 | Numerical model for quantification.** (a) Finite element simulations for fluid flow and deformation of an elastic sample calculated for vertical pipette positions corresponding to 99% ion current (top panel,  $z_0 = 1.6r_i$ ) and to 98% ion current (bottom panel,  $z = 0.4r_i$ ). (b) Vertical pipette position at 99% ion current,  $z_0$ , and at 98% ion current,  $z$ , as a function of sample compliance  $J$ .  $\delta_0$  denotes the difference between the two positions at zero sample compliance ( $J = 0$ ). (c) Relative sample deformation, defined as  $\delta = z_0 - z - \delta_0$ , as a function of  $J$  for different values of inner half cone angle  $\alpha$ . The parameters for the shown FEM simulations are  $J = 1.5 p_0^{-1}$  (panel a),  $\alpha = 4^\circ$  (panels a and b), and ratio of outer to inner opening radius  $r_o/r_i = 1.5$ . The dashed red traces denote linear fits (b) and fits of Equation (5) (c).

## Creep Compliance and Complex Modulus of Living Cells Follow a Power-Law Model



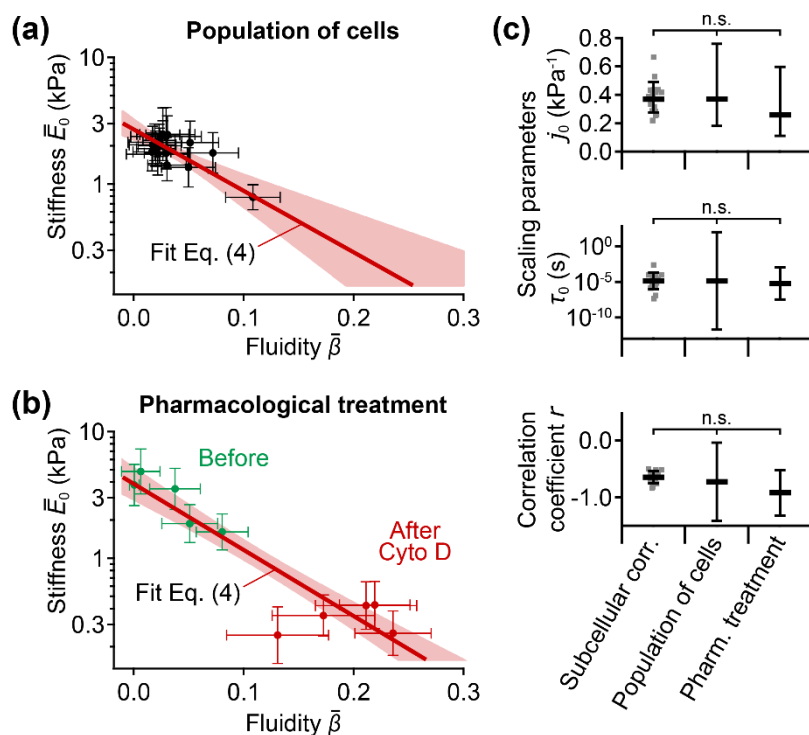
**Suppl. Fig. S-2 | Creep compliance and complex modulus of a living cell and power-law model.** (a) Creep compliance  $J(t)$  with a time relative to  $t_s$  (start of creep measurement) recorded on a living cell (same data as Figure 1c, bottom panel) shown on a log-log scale with fits of power law (Equation (3), red dashed trace), Maxwell [ $J(t) = E^{-1}(1 + t/\tau)$ , gives  $E = 2.9$  kPa and  $\tau = 0.23$  s, red dotted trace], and Kelvin-Voigt [ $J(t) = E^{-1}(1 - e^{-t/\tau})$ , gives  $E = 2.3$  kPa and  $\tau = 3.5$  ms, red dashed-dotted trace] models. Here,  $E$ ,  $\eta$ , and  $\tau = \eta/E$  denote modulus of elasticity, viscosity, and time constant, respectively. Interpreting the time constant in terms of a poroelastic material model<sup>1</sup> gives poroelastic diffusion constants of typically  $D_p = L^2/\tau \approx 10 \mu\text{m}^2\text{s}^{-1}$  (using  $L \approx r_i$  as characteristic length scale), consistent with AFM experiments.<sup>1</sup> (b) Complex modulus  $E^*(\omega) = E'(\omega) + i E''(\omega)$  calculated by the modified Fourier transform<sup>2</sup> of the creep compliance data (solid traces) and power-law model (red dashed-dotted trace, prediction from the fit in the time domain data).

## Verification on a Silicone Polymer Sample



**Suppl. Fig. S-3 | Verification on a silicone polymer sample.** Map of (a) sample height, (b) stiffness, and (c) fluidity recorded on a CY52-276 polymer with the nominal mixing ratio of 1: 1 (part A to part B). (d) Scatter plot of stiffness  $E_0$  vs. fluidity  $\beta$  and histograms of stiffness  $E_0$  (right) and fluidity  $\beta$  (top) with an indication of log-normal and normal distributions (black curves), respectively. As expected, the polymer is homogenous in stiffness and fluidity, within a narrow range of  $\bar{E}_0 = 28 \pm 1$  kPa and  $\bar{\beta} = 0.25 \pm 0.03$  (average  $\pm$  standard deviation). No strong correlation between  $E_0$  and  $\beta$  was observed. For a mixing ratio of 6: 5 (part A to part B) we measured averages  $\bar{E}_0 = 10$  kPa and  $\bar{\beta} = 0.4$ , which is in very good agreement with AFM data on the same polymer with a similar mixing ratio.<sup>3</sup> The applied pressure was  $p_0 = 150$  kPa. Scale bars: 5  $\mu\text{m}$  (a-c).

## Correlation for Cell Population and for Pharmacological Treatment

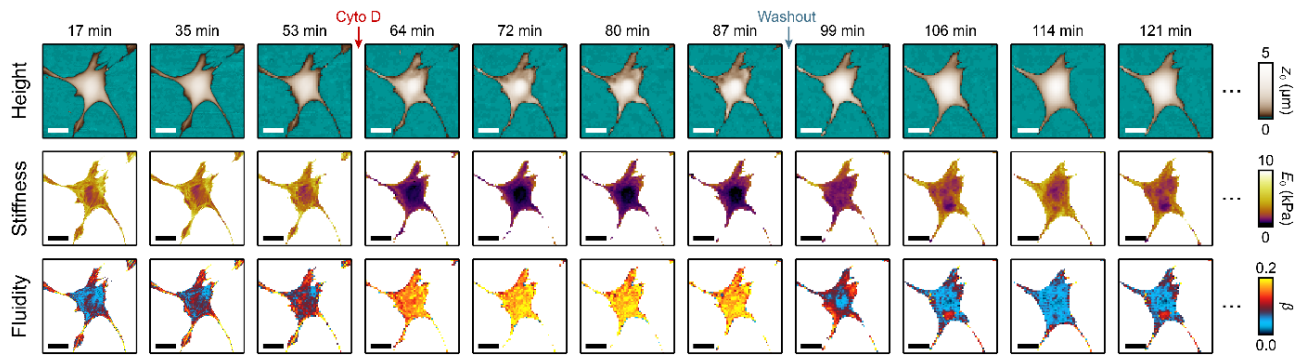


**Suppl. Fig. S-4 | Correlation between average stiffness and fluidity for the population of cells and for cells during pharmacological treatment. (a)** Average stiffness  $\bar{E}_0$  vs. average fluidity  $\bar{\beta}$  for the population of cells ( $N = 17$  cells) with fit of Equation (4) (red line). **(b)** Average stiffness  $\bar{E}_0$  vs. average fluidity  $\bar{\beta}$  for cells ( $N = 5$  cells) before and 30 min after pharmacological treatment with 2  $\mu$ M cytochalasin D with fit of Equation (4). **(c)** Average scaling parameters  $j_0$  and  $\tau_0$  and average correlation coefficient  $r$  obtained from subcellular correlations (see *e.g.* Fig. 3), from the population of cells (see panel a), and from pharmacological treatment (see panel b). Plots show average values (markers) and data of individual cells (dots); error bars indicate estimated standard deviation. The light red areas represent standard error of the fit (a, b).

**Table S1 |** Average scaling parameters  $j_0$  and  $\tau_0$  and average correlation coefficient  $r$  obtained from subcellular correlations (see *e.g.* Fig. 3), from the population of cells (see Suppl. Fig. S-4a), and from pharmacological treatment (see Suppl. Fig. S-4a), provided as average  $\ast$  (scaling parameters) or  $\pm$  (correlation coefficient) standard error.

	Scaling parameters		Correlation coefficient	Number of cells
	$j_0$ (kPa $^{-1}$ )	$\tau_0$ ( $\mu$ s)	$r$	$N$
Subcellular correlation	0.368 $\ast$ 1.1	13.2 $\ast$ 1.9	$-0.65 \pm 0.03$	17
Population of cells	0.371 $\ast$ 1.2	14.3 $\ast$ 60	$-0.72 \pm 0.18$	17
Pharmacological treatment	0.258 $\ast$ 1.3	6.01 $\ast$ 6.4	$-0.91 \pm 0.14$	5

## Stiffness and Fluidity of a Living Cell during Cytoskeleton Disruption and Recovery



**Suppl. Fig. S-5 | Stiffness and fluidity of a living cell during cytoskeleton disruption and recovery.** Whole sequence of topography images (top row) and maps of stiffness  $E_0$  (middle row) and fluidity  $\beta$  (bottom row) of the living fibroblast cell from Figure 4 during addition and washout of 2  $\mu\text{M}$  cytochalasin D. Scale bars: 20  $\mu\text{m}$ . See also Supplementary Video S1 for an animation of this sequence.

### References

- 1 E. Moendarbary, L. Valon, M. Fritzsche, A. R. Harris, D. A. Moulding, A. J. Thrasher, E. Stride, L. Mahadevan and G. T. Charras, *Nat. Mater.*, 2013, **12**, 253-261.
- 2 R. M. L. Evans, M. Tassieri, D. Auhl and T. A. Waigh, *Phys. Rev. E*, 2009, **80**, 012501.
- 3 R. Takahashi and T. Okajima, *Appl. Phys. Lett.*, 2015, **107**, 173702.